# Self-Induced Oscillations in Electronically-Coupled Fluxgate Magnetometers

Visarath In[*], Adi Bulsara[*], Andy Kho[*], Antonio Palacios[†], Patrick Longhini[†], Juan Acebron[**], Salvatore Aglio[‡] and Bruno Ando[‡]

[*]*Space and Naval Warfare Systems Center, Code 2363, 53560 Hull Street, San DIego, CA 92152-5001, USA*
[†]*Nonlinear Dynamics Group, Department of Mathematics and Statistics, San Diego State University, San Diego, CA 92182-7720, USA*
[**]*Dipartimento di Ingegneria dell' Informazione, Universita' di Padova, Via Gradenigo 6/B, 35131 Padova, ITALY*
[‡]*Dipartimento di Ingegneria Elettrica Elettronica e dei Sistemi, Univ. degli Studi di Catania, Viale A. Doria 6, 95125 Catania, ITALY.*

**Abstract.** We present theoretical and experimental investigations of the fundamental idea that coupling-induced oscillations can enhance the sensitivity of an array of magnetic sensors. In particular, we consider arrays made up of fluxgate magnetometers inductively coupled through electronic circuits. The underlying dynamics of the coupled system is more complicated as it shows new spatio-temporal features that are not observed in a single fluxgate. Among these new features, self-induced oscillations in the form of a traveling wave pattern are of particular interest because they can lead to higher sensitivity levels at reduced costs. Details of the experiments, a new signal detection mechanism, and results from numerical bifurcation analyzes are described in this work.

## INTRODUCTION

Fluxgate magnetometers are considered to be the most cost-efficient magnetic field sensors for applications that require measuring relatively small magnetic fields. For instance, measuring magnetic particles in biomedicine or in geological explorations. In either case, a single magnetometer operates (see next section for details) on the basis of saturation-driven oscillations generated by an external power source, so that an external signal is measured by quantifying its effect on the characteristics of the driven oscillations, i.e., changes in either the symmetry or the frequency of the wave form. Typically, a single fluxgate can measure magnetic fields in the range of about 1-10 $\mathrm{pT}/\sqrt{Hz}$ [1, 2]. Under current technology, greater sensitivity is only possible through the use of quantum-based sensors, though these sensors are far more complex and expensive. But now, motivated by new ideas and methods at the forefront of nonlinear dynamics in mathematics and physics, we show that it is possible for fluxgates to achieve higher levels of sensitivity. The basic ideas and methods are described next.

From the theoretical point of view, we first model the dynamics of an array of inductively coupled fluxgates through a system of differential equations. The system governs the magnetic induction in each fluxgate as a function of time. Then we perform a numerical bifurcation analysis to study the existence and stability of coupling-induced

CP742, *Experimental Chaos: 8th Experimental Chaos Conference,* edited by S. Boccaletti et al.

oscillations. Of particular interest are stable traveling wave (TW) patterns in which all fluxgates oscillate with the same waveform and same period but the oscillations are shifted by a constant amount. Then we show that the symmetry-breaking effect of an external signal is significantly stronger on the summed waveform of the self-induced oscillations than on each individual waveform. In this way, the sensitivity of fluxgate sensors can be enhanced by connecting them in arrays. From the experimental point of view, we first use printed circuit boards to build each individual fluxgate. Then we build electronic circuits to inductively couple the fluxgates in a manner that resembles the idealization of an array configuration. The experimental results are consistent with the theory, as they show that self-induced oscillations can enhance magnetic field sensitivity in an array of inductively coupled fluxgate magnetometers. Next we describe in more detail each of the tasks outlined above.

## A CLASSICAL FLUXGATE MAGNETOMETER

A classical fluxgate sensor consists of two identical ferromagnetic cores, each wound with an excitation coil oriented in opposite directions from one another, see Fig. 1. An alternating current drives the cores into saturation, creating induced magnetic fields of equal strength but with opposite orientations. A "pickup" coil surrounds the two ferromagnetic cores. The magnetic fields induced in the cores produce a voltage potential in the pickup coil, so that an external signal can be detected and measured by quantifying the voltage difference that it creates in the pick up coil. Fluxgates were originally developed for use as a submarine detection device for low-flying aircraft. Today, individual fluxgate devices can measure magnetic fields in the range of about 1-10 pT/$\sqrt{Hz}$ [1, 2] and they are used in applications such as: geophysical exploration, surveillance in land and sea, and underwater exploration [3, 4, 5, 6].

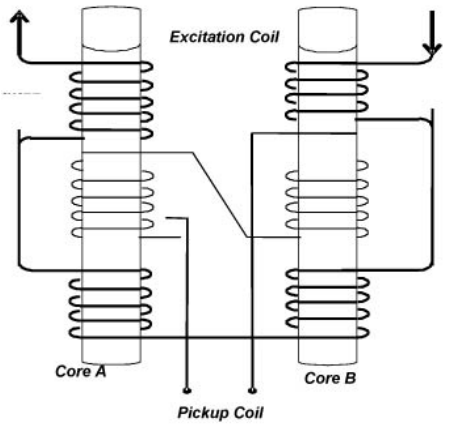


**FIGURE 1.** Schematic diagram of a classical fluxgate magnetometer.

## COUPLED FLUXGATE MAGNETOMETERS

At the center of our work is the idea of exploiting the phenomenon of *coupling-induced oscillations* [7, 8, 9] for signal detection enhancement in a network of coupled sensors. We have tested this idea using $N$ identical fluxgates coupled in a directed-ring through induction in the pickup coil (or the excitation coil). A model (with dimensionless variables) has the form

$$\frac{dx_i}{dt} = -x_i + \tanh(c(x_i + \lambda x_{i+1} + \varepsilon)), \qquad i = 1, \ldots, N \bmod N, \tag{1}$$

where $x_i(t)$ represents the magnetic flux in the pickup coil of the $i$-th unit, $c$ is a temperature-dependent parameter, $\varepsilon$ is the "target" magnetic field, and $\lambda$ is the coupling strength. For $c > 1$, each uncoupled ($\lambda = 0$) fluxgate is bistable. Absent an external force, i.e., $\varepsilon = 0$, $x_i(t)$ will relax to one of the two stable attractors at $x = \pm 1$. But for certain values of $N > 1$ a bifurcation analysis [8] shows, however, that each unit will oscillate about the two stable attractors with a symmetric waveform. See next section for details.

## BIFURCATION ANALYSIS

A simple numerical integration of (1) reveals oscillatory behavior for $\lambda < \lambda_c$, see Figure 2, where $\lambda_c$ is a critical (or threshold) value of the coupling strength [8]. The oscillations are non-sinusoidal, with a frequency that increases as the coupling strength decreases away from $\lambda_c$. For $\lambda > \lambda_c$, however, the system quickly settles into one of its steady states, regardless of the initial conditions; the same result ensues if $N$ is even, or if the coupling is bidirectional. As a side-note, we point out that the appearance of oscillations for $\lambda < \lambda_c$ does not violate any conservation laws; in a practical implementation, some onboard power (e.g. to drive the coupling circuit) is always present. The dc target signal $\varepsilon$ has the effect of skewing the potential function (for zero coupling) of each element. This has implications for the oscillation frequency as well as the residence times (or, equivalently, the zero-crossings) of individual elements of the connected array.

For even values of $N$ (and the same form of unidirectional coupling among nearest neighbors), the system also undergoes a series of Hopf bifurcations, but all of the branches are unstable and, hence, unobservable. While more specialized coupling schemes are beyond the purview of this paper, we have also investigated different coupling topologies that include: bidirectional coupling amongst nearest neighbors, unidirectional coupling for nearest neighbors combined with bidirectional coupling between non-nearest neighbors, and unidirectional coupling for nearest neighbors combined with unidirectional coupling between every other non-nearest neighbors. In all these cases, additional coupling facilitates the existence of oscillatory behavior but aside from a potential enhanced tolerance to background noise, increasing the number of elements or re-arranging the network to have a different coupling topology does not seem to increase performance as quantified, for example, by the sensitivity of the oscillation frequency to small changes in an applied dc target signal. In summary, from the application point of view, the $N = 3$ case is the simplest, and most relevant, case to realize.

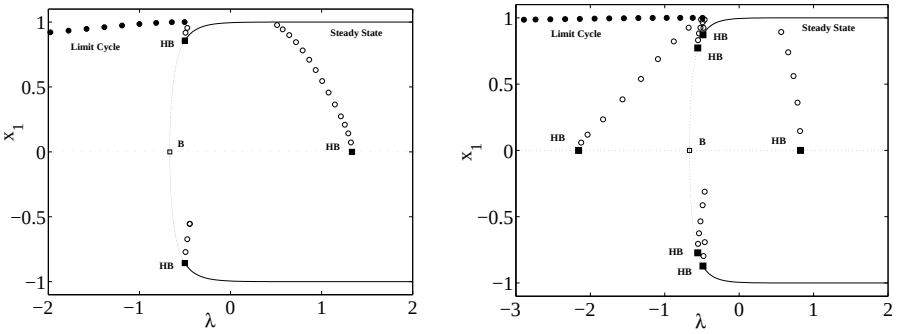


**FIGURE 2.** Bifurcation diagram for the coupled system of equations (1) with $N = 3$, $c = 3$, and $\varepsilon = 0$. Filled-in squares are local Hopf bifurcations to unstable periodic solutions (empty circles); empty square describes a steady-state pitchfork bifurcation point of two branches of nontrivial unstable equilibria (dotted lines). Filled-in circles represent stable periodic solutions created via global bifurcations.

## EXPERIMENTS

The experimental realization of the model equations (1) with $N = 3$ is shown in Figure 3, together with a block diagram that illustrates each stage of the coupling circuit. Each individual fluxgate is built through PCB (printed circuit board) technology. The ferromagnetic cores, in particular, are made of the Cobalt-based Metglas 2714A material. The sides of the PCB sheets that face away from the core material are printed with copper wirings to form the windings for the driving coil and the sensing coil. Solder is used to fuse the two sheets together to complete the circuit for the windings. The fluxgates are then coupled through an electronic circuit as follows. First, the (voltage) readout of one fluxgate signal (i.e. the derivative signal of the flux detected by the sensing coil of the device) is amplified by a voltage amplifier (an instrumentation amplifier with a very high impedence). At this point the amplifier also trims out any dc in the output. Then the signal is passed through a “leaky” integrator to convert the derivative signal seen by the sensing coil back to the “flux” form so that the experimental system closely conforms to the model (1). The use of a "leaky" integrator helps avoid the divergence caused by a small dc signal that might have gotten through the voltage amplifier stage. Typically the output of an integrator is also accompanied by dc that must be removed before the signal is passsed to the other fluxgates. This is accomplished by employing a Sallen-Key second-order high pass filter immediately after the integrator, with the parameters tuned to work at a specific frequency (the mean oscillating frequency of the coupled system). The signal then passes through an amplifier to achieve adequate gain to drive the adjacent fluxgate. After this step, the signal passes through a voltage-to-current converter (V-I converter) in its final route to drive the primary coil of the adjacent fluxgate. This converter also has a gain factor but it is fixed to a certain value during the construction of the coupling circuits. The gain is set at much less than unity so that one volt in the signal does not convert to one ampere in the voltage-to-current converter stage. The same setup is repeated for the other two coupling connections of the remaining fluxgates, and

all values of the coupling circuit parameters are closely matched from one set to the other. Each stage of the coupling circuit also employs high speed and high precision operational amplifiers to minimize the time delay in order to conform closely to the model since knowledge of state variable $x_i$ is known instantly in the model.

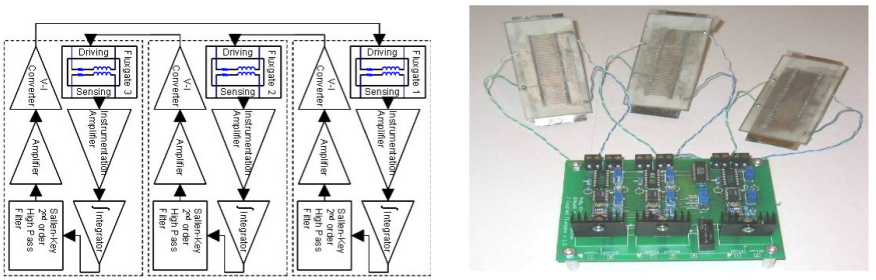


**FIGURE 3.** (Left) Block diagram of coupling circuit for creating an array of three coupling-induced fluxgate magnetometers; (right) actual prototype device.

The system readily oscillates in a traveling wave pattern, see Figure 4. As in the model, the system favors this pattern no matter how many times it is restarted. The frequency of oscillations is about 57 Hz. Each wave is phase shifted by exactly $\frac{2\pi}{3}$ as predicted by the model. Further comparisons with numerical results show good agreement with the characteristics of the oscillations. Both waveforms are qualitively similar but the waveform from the experiment is a mirror image of the waveform from the model. This is probably due to the inversion of the winding of the coils in the construction of the fluxgates.

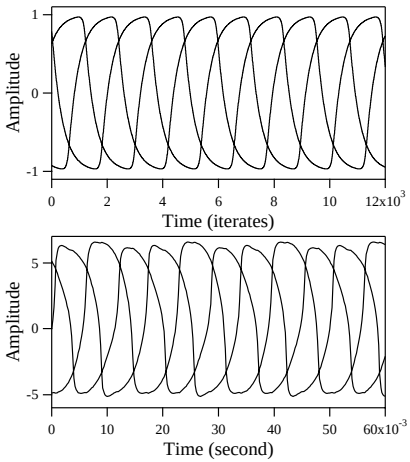


**FIGURE 4.** (Top): Coupling-induced oscillations obtained in simulations of an array of three fluxgates through (1) with $c = 4$, $\lambda = -1.55$, and $\varepsilon = 0$. (Bottom) Results from equivalent experimental system.

In addition, since we do not know the exact value of the parameter $c$ and a time constant $\tau$, which arises in the derivation of (1), in the actual device (we set $\tau = 1$ in the

model), we cannot correctly compare the time scales in the model and the experimental observations. The amplitudes of the oscillations in the experiment are also arbitrary compared to the model because the recorded voltages depend on the gains set in the coupling circuit. On the other hand, the magnetic flux in the model saturates between $\pm 1$, but in the fluxgate devices, this quantity cannot be measured directly. To measure an external signal, we quantify its symmetry-breaking effect through the residence times (RT) ratio around the stable attractors $\pm 1$. The critical observation is that the RT ratio in a ring of three fluxgates is about 400 times the RT ratio of a single fluxgate. In other words, the ring is (theoretically) three orders of magnitude more sensitive than a single fluxgate. RT ratio curves are not included in this paper for brevity. In practice, the amount of sensitivity enhancement (without optimization) is about 100 times better. The exact experimental limit of enhancement is part of on-going work.

## ACKNOWLEDGMENTS

The authors acknowledge support from the Office of Naval Research (Code 331). PL and AP were supported in part by the San Diego State Foundation Grant C-2003-00307.

## REFERENCES

1. Karlsson, M., Robinson, J., Gammaitoni, L., and Bulsara, A., "The optimal achievable accuracy of the Advanced Dynamic Fluxgate Magnetometer (ADFM)," in *Proceedings of MARELEC*, Stockholm, Sweden, 2001.
2. Koch, R., Deak, J., and Grinstein, G., *Applied Physics Letters*, **75**, 3862–3864 (1999).
3. Gordon, D., and Brown, R., *IEEE Trans. Magnetics*, **MAG-8**, 76–82 (1972).
4. Lenz, J., "A review of magnetic sensors," in *Proceedings IEEE*, 1990, vol. 78, p. 973.
5. Russell, C., Elphic, R., and Slavin, J., *Science*, **203**, 745 (1979).
6. Snare, R., and Means, J., *IEEE Trans. Magnetics*, **MAG-13**, 1107–1977 (1997).
7. Bulsara, A., In, V., Kho, A., Longhini, P., Palacios, A., Rappel, W., Acebron, J., Baglio, S., and Ando, B., *Physical Review E* (2004), in press.
8. In, V., Bulsara, A., Palacios, A., Longhini, P., Kho, A., and Neff, J., *Physical Review E*, **68**, 045102–1–0415102–4 (2003).
9. In, V., Kho, A., Neff, J., Palacios, A., Longhini, P., and Meadows, B., *Physical Review Letters*, **91**, 244101–1–244101–4 (2003).